J. Phys. Chem. A **2008,** *112,* 3953−3958

The Destruction of Atmospheric Pressure Propane and Propene Using a Surface Discharge Plasma Reactor

Sarah L. Hill,[†] Hyun-Ha Kim,[‡] Shigeru Futamura,[‡] and J. Christopher Whitehead*,[†]

School of Chemistry, The University of Manchester, Oxford Road, Manchester M13 9PL, United Kingdom, and National Institute of Advanced Industrial Science and Technology (AIST), AIST Tsukuba West, 16-1 Onogawa, Tsukuba, Ibaraki 305-8569, Japan

Received: January 8, 2008; In Final Form: February 5, 2008

Surface discharge plasma reactors (SDRs) have been shown to be effective in removing a wide range of pollutants. In this study, the effectiveness of a SDR for the removal of propane and propene from an atmospheric pressure air stream was investigated. For an input energy of 100 J L^{-1}, the conversions were found to be 16% and 68% for propane and propene, respectively. The total carbon recovery was found to increase with increasing specific input energy (SIE) for both hydrocarbons. FTIR analysis showed that CO and CO_2 are the major end-products, and GC−MS identified formic acid as a significant byproduct. The effect of initial propane concentration was also investigated. The reaction chemistry involved in the oxidative plasma conversion of propane and propene is discussed.

Introduction

Non-thermal plasma discharges offer a new method for processing waste gas and are especially efficient for the removal of volatile organic compounds (VOCs) at low concentration levels. Surface discharge reactors (SDRs) have been shown to be highly effective at producing ozone; a configuration of ceramic tube with internal strip electrodes can produce up to 30 000 ppm of ozone from a pure oxygen stream when an AC voltage of 10 kHz and 5 kV is applied. A major use for this type of reactor is the sterilization of surgical instruments.[1] More recently, SDRs have been used successfully to remove a variety of pollutants ranging from alcohols and aldehydes to aromatics and halogenated hydrocarbons. Oda et al.[2] find removal rates of 95% for acetone and 100% for 2-propanol using a ceramic tube reactor with strip-like electrodes and input powers of 30 and 15 W, respectively. Halogenated hydrocarbons can be removed with efficiencies up to 50% as shown by Ogata et al.[3] and up to 80% as documented by Oda et al.[4] High carbon balances, up to 90%, have also been recorded by Oh et al.[5] during successful decomposition of toluene. Product analysis shows that the majority of the destroyed toluene is converted to CO and CO_2 with trace amounts of formic acid also detectable.

In this study, the removal of propane and propene from waste gas streams is investigated using a SDR. Previous work by Jarrige and Vervisch[6] has reported the destruction of propane and propene in air with a pulsed corona discharge at atmospheric pressure. They found that with a specific input energy, SIE (electrical power supplied to the plasma/gas flow rate), of 100 J L^{-1}, 95% of propene was destroyed as compared to only 10% of propane.

Experimental Section

A schematic diagram of the setup used can be found in Figure 1. Experiments were carried out using a surface discharge reactor (SDR), comprised of a quartz tube (i.d. of 9 mm and length of 160 mm), the outside of which is coated in silver paint to act as a grounded electrode. The high voltage electrode is a stainless steel wire coiled on the inside of the tube. The arrangement of electrodes is shown in cut-way form in Figure 1. This type of surface discharge reactor behaves in many ways like a dielectric barrier discharge where one of the electrodes just lies on the dielectric tube but the configuration results in a decrease in the breakdown voltages.[7] The flow of gas to the reactor was controlled using mass flow controllers (Flow Compo). Separate cylinders of 1000 ppm propane in nitrogen and 1000 ppm propene in nitrogen (Takachiho Chemical Industrial Co. Ltd.) were used and diluted with synthetic air (80% N_2:20% O_2) at atmospheric pressure to give initial concentrations of 100 ppm with an overall flow rate of 1 L min^{-1}. In separate experiments, the propane initial concentrations were increased to 300 and 400 ppm, while the overall flow remained at 1 L min^{-1}. A Perkin-Elmer Spectrum One FTIR detection system fitted with a long path gas cell (Gemini Scientific Instruments, VENUS gas cell 0.75 L/6.4 m path length) calibrated appropriately was used to analyze the end-products. An AC voltage was applied to produce the discharge, the frequency was varied between 50 Hz and 1 kHz, and the peak−peak voltage was varied from 14 to 32 kV. Using a digital storage oscilloscope (Tektronix TDS

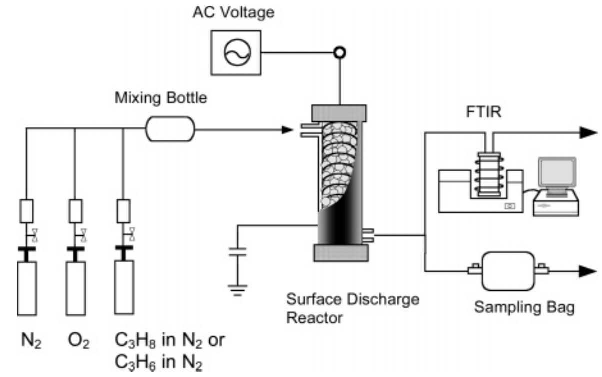

Figure 1. A schematic diagram of the experimental setup used.

---

* Corresponding author. E-mail: j.c.whitehead@manchester.ac.uk.

[†] The University of Manchester.

[‡] National Institute of Advanced Industrial Science and Technology.

10.1021/jp800146t CCC: $40.75

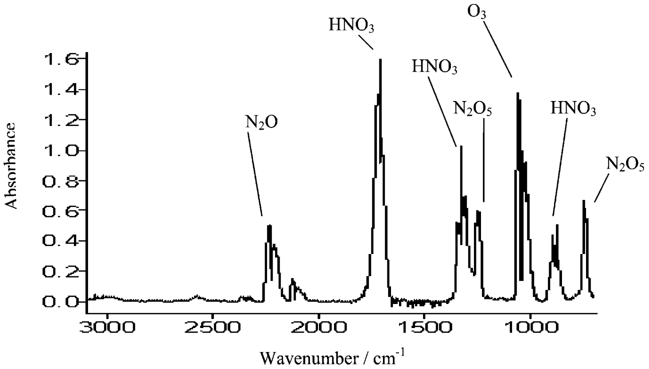

Figure 2. IR spectrum for humid air using SDR with SIE = 625 J L^{-1}.

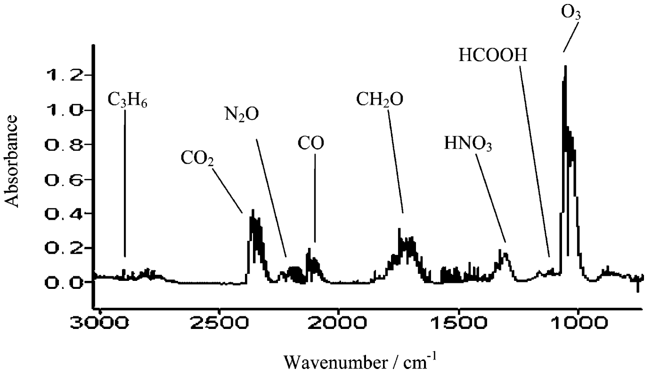

Figure 3. IR spectrum for 70% propene destruction in humid air using SDR with SIE = 89 J L^{-1}.

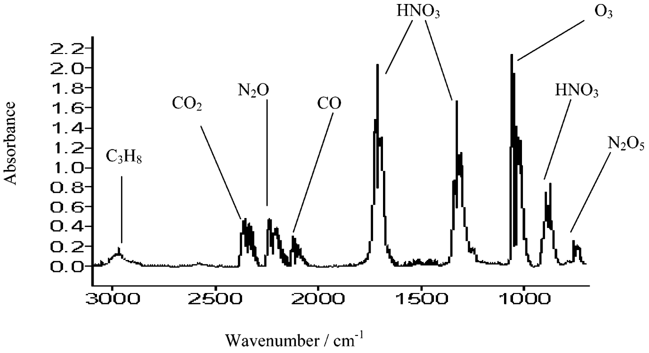

Figure 4. IR spectrum for 62% propane destruction in humid air using SDR with SIE = 680 J L^{-1}.

3034B), the current and voltage waveforms of the discharge were recorded using calibrated high voltage probes. The computer program used to measure the power is the voltage-charge Lissajous Programme (version 1.4) described previously.[8,9] From the calculated power the specific input energies, SIE, can be obtained by dividing the power by the flow rate; these were found to be in the range of 14−930 J L^{-1}. A sampling bag was incorporated into the system to allow gas samples to be withdrawn for GC−MS (Shimadzu GC-17 with DB1 column) analysis of the byproducts.

Results and Discussion

Figures 2−4 show the IR spectra obtained for the SDR processing of air only, propene in air, and propane in air, respectively. The major products of air processing are N_2O, O_3, HNO_3, and N_2O_5; concentrations can be found in Table 1. The addition of propane produces CO and CO_2 as products, and the addition of propene gave CO, CO_2, CH_2O, and HCOOH as products as well as the products obtained for processing in air.

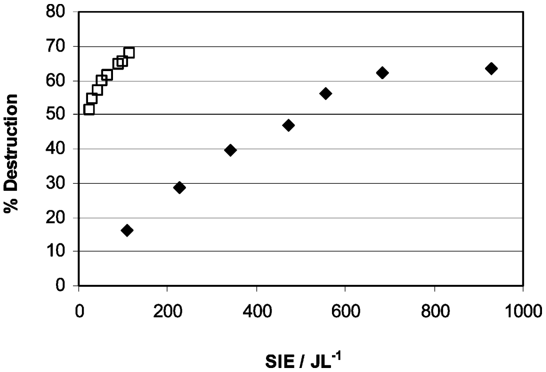

Figure 5. The destruction of propane and propene in a SDR as a function of SIE. ◆ propane; □ propene.

TABLE 1: Products from SDR Processing of Air

SIE/J L^{-1}	N_2O/ppm	O_3/ppm	HNO_3/ppm	N_2O_5/ppm
103	17	685	47	6
214	40	1297	87	18
435	77	1054	159	58
625	105	533	228	103
950	121	5	233	141

These concentrations are shown in Table 2. Figure 5 shows how the destruction of each hydrocarbon is affected by the SIE; an increase in SIE increases the % conversion in both cases.

Figure 2 shows the IR spectrum of the products from the SDR processing of air, containing ≤100 ppm water vapor, which were found to be N_2O, O_3, HNO_3, and N_2O_5. Large amounts of ozone are typical of this type of reactor as is the presence of N_2O; their mechanism of production will be discussed later. Recording quantities of HNO_3 and N_2O_5 without also detecting NO or NO_2 is unusual. The route to produce HNO_3 and N_2O_5 starts with the formation of NO from reaction of molecular oxygen with nitrogen atoms formed from direct electron impact dissociation of N_2 in the plasma discharge:

$$N + O_2 \rightarrow NO + O \tag{1}$$

Because of the heavily oxidative environment of the SDR, dominated by ozone, the NO is swiftly converted to NO_2

$$NO + O_3 \rightarrow NO_2 + O_2 \tag{2}$$

and to a lesser extent by the reaction

$$O + NO + M \rightarrow NO_2 + M \tag{3}$$

This NO_2 can react further with oxygen atoms, formed from direct electron impact dissociation of O_2 in the plasma discharge to produce NO_3. Alternatively, NO_2 can react with hydroxyl radicals created by plasma destruction of water to produce HNO_3, which is a product seen on the IR spectrum. Both of these processes are third-order reactions.

$$NO_2 + O + M \rightarrow NO_3 + M \tag{4}$$

$$NO_2 + OH + M \rightarrow HNO_3 + M \tag{5}$$

The NO_3 can react with NO_2 to create N_2O_5, another product seen on the IR spectrum, in a three-body reaction:

$$NO_3 + NO_2 + M \rightarrow N_2O_5 + M \tag{6}$$

As we do not detect NO or NO_2, reactions 2−6 must proceed rapidly, removing all NO and NO_2 from the system.

TABLE 2: Products from SDR Processing of 100 ppm Propane and 100 ppm Propene in Air

	SIE /J L^{-1}	hydrocarbon /ppm	CO /ppm	CO_2 /ppm	N_2O /ppm	O_3 /ppm	HNO_3 /ppm	N_2O_5 /ppm	HCHO /ppm	HCOOH /ppm
propane	109	82	17	0	15	635	43	0	0	0
	226	70	27	10	36	1014	90	0	0	0
	342	59	41	24	53	924	140	0	0	0
	473	52	58	38	70	1130	189	0	0	0
	556	43	78	48	85	1476	237	0	0	0
	682	37	95	57	99	732	267	31	0	0
	930	36	112	63	116	47	279	124	0	0
propene	24	49	14	34	0	141	10	0	32	12
	32	46	19	36	0	192	13	0	33	13
	43	43	26	40	0.1	274	17	0	32	13
	52	40	30	43	1.1	314	20	0	32	13
	65	39	37	48	3.7	393	25	0	30	14
	89	35	47	56	7.8	511	33	0	28	14
	100	35	52	63	10	547	39	0	28	15
	114	32	55	65	12	594	41	0	26	15

TABLE 3: Rates of Reactions between Propane/Propene and O/OH Radicals at 400 K[a]

compound	type of reaction	reaction with	equation	rate expression ($cm^3\ mol^{-1}\ s^{-1}$)
propane	H abstraction	O	$C_3H_8 + O \Rightarrow n\text{-}C_3H_7 + OH$	1.69×10^{10}
			$C_3H_8 + O \Rightarrow i\text{-}C_3H_7 + OH$	3.80×10^{10}
		OH	$C_3H_8 + OH \Rightarrow n\text{-}C_3H_7 + H_2O$	4.71×10^{11}
			$C_3H_8 + OH \Rightarrow i\text{-}C_3H_7 + H_2O$	1.06×10^{12}
propene	H abstraction	O	$C_3H_6 + O \Rightarrow CH_3CCH_2 + OH$	2.71×10^{8}
			$C_3H_6 + O \Rightarrow CH_3CHCH + OH$	1.01×10^{8}
			$C_3H_6 + O \Rightarrow CH_2CHCH_2 + OH$	7.08×10^{9}
		OH	$C_3H_6 + OH \Rightarrow CH_3CCH_2 + H_2O$	2.86×10^{10}
			$C_3H_6 + OH \Rightarrow CH_3CHCH + H_2O$	1.03×10^{10}
			$C_3H_6 + OH \Rightarrow CH_2CHCH_2 + H_2O$	7.26×10^{11}
	fragmentation	O	$C_3H_6 + O \Rightarrow HCO + C_2H_5$	1.09×10^{12}
			$C_3H_6 + O \Rightarrow CH_2COH + CH_3$	7.86×10^{11}
			$C_3H_6 + O \Rightarrow OCCH_2 + CH_3 + H$	5.24×10^{12}
		OH	$C_3H_6 + OH \Rightarrow CH_3CHO + CH_3$	1.71×10^{14}
			$C_3H_6 + OH \Rightarrow CH_2O + C_2H_5$	1.95×10^{14}
	addition to double bond	O	$C_3H_6 + O \Rightarrow$ methyloxirane	2.23×10^{12}
		OH	$C_3H_6 + OH + M \Rightarrow C_3H_6OH + M$	1.03×10^{21} [b]

[a] All values taken from NIST Chemical Kinetics Database website.[18] [b] Units are $cm^6\ mol^{-2}\ s^{-1}$.

TABLE 4: The CO and CO_2 Selectivities and the Total Carbon Recovery from the Destruction of Propane and Propene in SDR

propane				propene			
	% selectivity				% selectivity		
SIE/J L^{-1}	CO	CO_2	% total carbon recovery	SIE/J L^{-1}	CO	CO_2	% total carbon recovery
100	34	0	34	20	22	9	31
200	33	12	45	30	22	12	24
300	35	21	56	40	23	15	38
400	42	27	69	50	24	17	41
500	47	29	76	60	26	20	46
700	52	31	83	90	29	24	53
900	60	34	94	100	32	27	59

Propane and Propene Destruction. The destruction of propene requires far less SIE than does propane to obtain comparable destructions. Over 10 times as much energy is needed to obtain a 60% destruction of propane as for propene. To explain these results, the reactions of the hydrocarbons with the plasma-produced species must be discussed. Figure 4 shows the IR spectrum after the destruction of propane in air using SDR. The result is quite similar to an air plasma, Figure 2, but more HNO_3 is created and less N_2O_5. This is to be expected as propane destruction will add more OH radicals to the processing, thus increasing the rate of HNO_3 production via reaction 5. In addition, peaks for CO and CO_2 are detected, resulting from the oxidation of the hydrocarbon. Figure 4 shows the IR spectrum for the processing of propene in air, which is very different from the previous two spectra. Despite a similar level of destruction (62% and 70% for propane and propene, respectively), the concentration of HNO_3 is significantly lower and other minor products are detected including formaldehyde, CH_2O, and formic acid, HCOOH. The lack of HNO_3 is almost certainly due to the much lower SIE range (up to 114 J L^{-1} as compared to 930 J L^{-1}) giving less NOx and thus less HNO_3. The presence of CH_2O and HCOOH shows that there are different removal pathways for propene destruction as compared to propane and that oxidation is less complete at lower SIE.

Initially the only plasma-produced species capable of reacting with propane or propene are oxygen atoms, which are primary radicals, created directly in the plasma by electron impact reactions with oxygen molecules. Propane, being a saturated hydrocarbon, can only undergo hydrogen atom abstraction with these oxygen atoms:

$$C_3H_8 + O \rightarrow n\text{-}C_3H_7 + OH \tag{7}$$

$$C_3H_8 + O \rightarrow i\text{-}C_3H_7 + OH \tag{8}$$

The unsaturated nature of the propene molecule allows for a greater variety of oxygen atom reactions to occur in addition to hydrogen atom abstraction, in particular, addition to the double bond and fragmentation reactions.

$$C_3H_6 + O \rightarrow C_3H_5 + OH \tag{9}$$

$$C_3H_6 + O \rightarrow HCO + C_2H_5 \tag{10}$$

$$C_3H_6 + O \rightarrow CH_2COH + CH_3 \tag{11}$$

$$C_3H_6 + O \rightarrow OCCH_2 + CH_3 + H \tag{12}$$

$$C_3H_6 + O \rightarrow \text{methyloxirane} \tag{13}$$

These removal pathways are also documented by Dorai and Kushner[10] in Figure 1 of their paper.

Despite hydrogen abstraction rates for propene being lower than propane, see Table 3, the cumulative rate of propene reactions with oxygen atoms is larger due to the additional reactions involving the C=C, some of which have rates in the order of 10^{12} cm^3 mol^{-1} s^{-1}.

Subsequently further active species, which are secondary radicals such as OH, can be generated by reactions such as (7)–(9) and can also react with the C3 hydrocarbons. The only route available for the reaction of OH with propane is again hydrogen atom abstraction:

$$C_3H_8 + OH \rightarrow n\text{-}C_3H_7 + H_2O \tag{14}$$

$$C_3H_8 + OH \rightarrow i\text{-}C_3H_7 + H_2O \tag{15}$$

In contrast, propene has a variety of reaction routes available due to the reactivity of the double bond:

$$C_3H_6 + OH \rightarrow C_3H_5 + H_2O \tag{16}$$

$$C_3H_6 + OH \rightarrow CH_3CHO + CH_3 \tag{17}$$

$$C_3H_6 + OH \rightarrow CH_2O + C_2H_5 \tag{18}$$

$$C_3H_6 + OH + M \rightarrow C_3H_6OH + M \tag{19}$$

Once again, the cumulative effect of all of these processes produces an overall rate substantially faster than that for propane. All of the possible reactions and their associated rates are detailed in Table 3.

Jarrige and Vervisch[6] observed similar differences between propane and propene during a study into their removal from an atmospheric pressure air stream using a pulsed corona discharge reactor. For a 60% level of destruction, 40 J L^{-1} was required for propene removal whereas propane requires 440 J L^{-1}. They attribute this difference to the reaction rates of the propane and propene with atomic oxygen, O(^{3}P).

From Table 3, it can be seen that these reactions lead to the production of radicals such as C_2H_5 and CH_3 as well as oxidative intermediates and byproducts such as acetaldehyde, formaldehyde, methyloxirane, and propanol. Some of these reactions are more important than others. Work undertaken by Martin et al.[11] on the plasma destruction of propene in simulated diesel exhaust shows that acetaldehyde and formaldehyde are major byproducts but substances like methyloxirane and propanol were not detected.

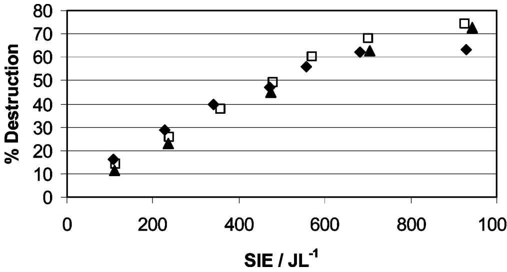

Figure 6. Propane destruction in SDR with varying initial concentration as a function of SIE. ◆ 100 ppm, ☐ 300 ppm, and ▲ 400 ppm.

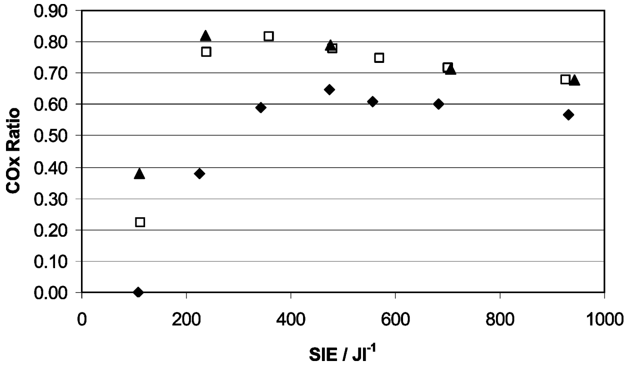

Figure 7. CO*x* ratio from the destruction of propane in SDR varying initial concentration as a function of SIE. ◆ 100 ppm, ☐ 300 ppm, and ▲ 400 ppm.

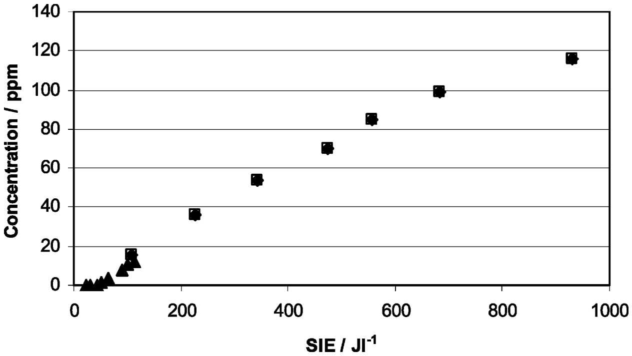

Figure 8. The production of N_2O in SDR as a function of SIE. ◆ air only, ☐ 100 ppm propane in air, and ▲ 100 ppm propene in air.

CO and CO$_2$ Selectivity. The selectivity for the production of CO or CO$_2$ is defined as the CO or CO$_2$ concentration as a percentage of the total carbon available from the hydrocarbon destroyed. The selectivities are given by:

$$\%\ \text{CO selectivity} = [\text{CO}]/(3 \times [\text{removed hydrocarbon}]) \times 100$$

$$\%\ \text{CO}_2\ \text{selectivity} = [\text{CO}_2]/(3 \times [\text{removed hydrocarbon}]) \times 100$$

These are listed in Table 4 and show that both compounds exhibit a larger selectivity for CO formation than for CO$_2$ over the whole SIE range. At a comparable SIE of 100 J L^{-1}, the total carbon recovery (i.e., the amount of converted carbon detected as either CO or CO$_2$) is better for propene than for propane. A possible explanation for this is given by Kim et

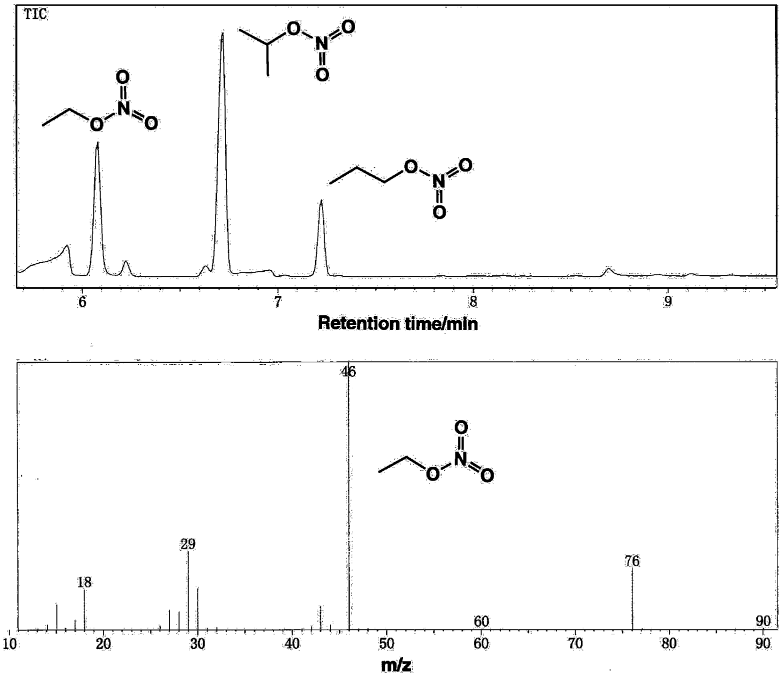

Figure 9. Chromatogram showing peaks of ethyl nitrate, and 1- and 2-propyl nitrate, and a mass spectrum of ethyl nitrate from SDR processing of propane in air.

TABLE 5: Total Carbon Recovery from the Destruction of Propane in Air with SDR as a Function of Initial Concentration

	initial concentration of propane		
SIE/J L^{-1}	100 ppm	300 ppm	400 ppm
100	34.4%	18.7%	21.7%
230	44.9%	32.4%	32.5%
475	69.4%	51.6%	49.9%
700	82.8%	62.2%	61.6%
930	94.1%	73.4%	71.2%

al.[12] who point out that the major route for CO_2 production in a plasma discharge is via reaction of OH with CO:

$$CO + OH \rightarrow CO_2 + H \tag{20}$$

At 100 J L^{-1}, only 16% of propane is removed as compared to 65% of propene. Larger hydrocarbon destruction implies that more OH radicals are available to convert CO to CO_2 via reaction 20 in the case of propene. The total carbon recovery increases with increasing SIE for both hydrocarbons, reaching 94% at high SIE for propane. High SIE will create more primary oxygen radicals, which promote complete oxidation to CO and CO_2 and hence increase the total carbon recovery.

Effect of Initial Concentration on Destruction and Selectivities. Altering the initial concentration of propane shows no appreciable difference in the propane destruction, Figure 6. However, a difference is observed in the CO and CO_2 production; Figure 7 shows the CO*x* ratio (CO_2:CO) as a function of SIE. A low initial concentration of propane (100 ppm) gives rise to a lower CO*x* ratio, indicating substantially more CO is produced than CO_2. The CO*x* ratios for 300 and 400 ppm initial concentrations are very similar, indicating more OH radicals available to convert CO to CO_2. The total carbon recovery increases with increasing SIE, Table 5, where 94% of carbon is accounted for with an initial concentration of 100 ppm as compared to ~70% for an initial concentration of 300 or 400 ppm at a high SIE of 900 J L^{-1}.

Nitrogen Oxides and Ozone Chemistry. NO*x* production in plasma is strongly dependent on the electric field strength. Penetrante has shown that at low electric field strengths electron impact processes favor oxygen dissociation and as the field is increased nitrogen dissociation routes become more important.[13] The low breakdown voltages involved with the SDR configuration imply that low electric field strengths are used,[7] which minimize N_2 dissociation and thus minimize the formation of NO via reaction 1. N_2O is produced via excited N_2, which is still formed in a low electric field:

$$N_2^* + O \rightarrow N_2O \tag{21}$$

In Figure 8, we see that N_2O production increases with SIE reaching 120 ppm at ~900 J L^{-1}, regardless of the hydrocarbon. As O_2 dissociation is predominant within a SDR, ozone production occurs during all experiments irrespective of the hydrocarbon used. Its concentration increases with increasing SIE to a broad maximum (~1400 ppm) at ~400 J L^{-1} but then falls to zero at ~1000 J L^{-1}. This pattern of ozone production has also been reported by Yamamoto[14] and Jarrige and Vervisch[6] who observe an initial increase in ozone as the applied voltage or SIE is raised, which then peaks and decreases at higher applied voltages or SIE. This behavior is a well-known phenomenon in air-fed ozonizers sometimes described as “discharge poisoning” where catalytic cycles involving NO and NO_2 lead to removal of atomic oxygen and ozone.[15]

GC−MS Analysis of Minor End Products. To investigate minor end products not detected by FTIR, samples of gas postprocessing (300 ppm of propane processed at 980 J L^{-1} and 300 ppm of propene processed at 370 J L^{-1}) were collected and GC−MS analysis was carried out. This was a qualitative analysis only. For both propane and propene, the following products were detected: acetone, formic acid, methyl nitrate, nitromethane, acetic acid, $C_2H_5NO_3$, $C_2H_5NO_2$, propyl nitrate, and isopropyl nitrate. Despite being unable to quantify the byproducts in this analysis, it is clear from the chromatograms that formic acid is a significant trace byproduct. Figure 9 shows an example of the chromatogram recorded and the MS spectra identified as $C_2H_5NO_3$.

The detection of nitrate and nitrite compounds albeit at a very low level is significant and has been observed previously. Dorai and Kushner[10,16] have shown that the production of alkyl nitrites and nitrates is responsible for the reduction of NO*x* during plasma processing of gas mixtures simulating diesel exhaust containing propane, propene, and NO in humid air. Conversely, Martin et al.[11] were able to process propene in dry air with an initial NO concentration of 500 ppm without the formation of methyl nitrate. We have previously reported[17] that during DBD processing of propane in air, nitrate and nitrite production is unimportant. This may be due to the difference in available NO and NO_2; Dorai and Kushner[10] use an initial NO concentration of 260 ppm, while our previous work[17] and the current work do not add NO to the gas stream, and thus the NO*x* available for reaction is only what is created in the air plasma discharge. The current work uses a SDR that produces undetectable levels of NO and NO_2, so it follows that the lack of available NO*x* in the discharge may limit the production of nitrate and nitrite compounds so that they are only qualitatively detectable with GC−MS and not with FTIR. Jarrige and Vervisch[6] also report the production of methyl nitrate, without NO*x* production, using FTIR detection when removing propane from air with a corona discharge. They hypothesize that the conventional methyl nitrate production route from methoxy radical reaction with NO_2 cannot occur, due to the lack of NO*x*, and that excited nitrogen molecules and atoms are involved by insertion into organic intermediates.

Conclusions

Using a SDR, percentage conversions of up to 70% can be achieved for both propane and propene. The destruction of propane requires substantially larger SIE as compared to propene; this is due to the limited number of available pathways to initiate propane removal. The destruction of propane is unaltered when the initial concentration is varied; however, a difference is observed in the selectivity of the products. More CO is produced at a low initial concentration of hydrocarbon. GC−MS analysis detected other carbon-containing byproducts, which included various alkyl nitrite and nitrate and small organic acids.

Acknowledgment. Support of this work by the UK Engineering and Physical Sciences Research Council and The Japan Society for the Promotion of Science is gratefully acknowledged.

References and Notes

(1) Masuda, S.; Kiss, E.; Ishida, K.; Asai, H. *IEEE Trans. Ind. Appl.* **1990**, *26*, 36.
(2) Oda, T.; Yamashita, R.; Haga, I.; Takahashi, T.; Masuda, S. *IEEE Trans. Ind. Appl.* **1996**, *32*, 118.
(3) Ogata, A.; Kim, H.-H.; Futamura, S.; Kushiyama, S.; Mizuno, K. *Appl. Catal., B: Environ.* **2004**, *53*, 175.
(4) Oda, T.; Takahashi, T.; Nakano, H.; Masuda, S. *IEEE Trans. Ind. Appl.* **1993**, *29*, 787.
(5) Oh, S.-M.; Kim, H.-H.; Ogata, A.; Einaga, H.; Futamura, S.; Park, D.-W. *Catal. Lett.* **2005**, *V99*, 101.
(6) Jarrige, J.; Vervisch, P. *J. Appl. Phys.* **2006**, *99*, 113303.
(7) Fridman, A. A.; Kennedy, L. A. *Plasma Physics and Engineering*, 1st ed.; Taylor & Francis, New York, 2004.
(8) Kim, H.-H.; Ogata, A.; Futamura, S. *IEEE Trans. Plasma Sci.* **2006**, *34*, 984.
(9) Harling, A. M.; Kim, H.-H.; Futamura, S.; Whitehead, J. C. *J. Phys. Chem. C* **2007**, *111*, 5090.
(10) Dorai, R.; Kushner, M. *J. Appl. Phys.* **2000**, *88*, 3739.
(11) Martin, A. R.; Shawcross, J. T.; Whitehead, J. C. *J. Phys. D: Appl. Phys.* **2004**, *37*, 42.
(12) Kim, H.-H.; Kobara, H.; Ogata, A.; Futamura, S. *IEEE Trans. Ind. Appl.* **2005**, *41*, 206.
(13) Penetrante, B. M. *Non-Thermal Plasma Techniques for Pollution Control. Part A: Overview, Fundamentals and Supporting Technologies* **1993**, 65.
(14) Yamamoto, T. *Journal of Electrostatics Selected Papers from the 1996 Joint IEJ/ESA Symposium on Electrostatics* **1997**, *42*, 227.
(15) Yagi, S.; Tanaka, M. *J. Phys. D: Appl. Phys.* **1979**, *12*, 1509.
(16) Dorai, R.; Kushner, M. J. *J. Phys. D: Appl. Phys.* **2001**, *34*, 574.
(17) Hill, S. L.; Whitehead, J. C.; Zhang, K. *Plasma Processes Polym.* **2007**, *4*, 710.
(18) NIST. Chemical Kinetics Database on the Web, Standard Reference Database 17, Version 7.0 (Web Version), Release 1.4, 2007, http://kinetics.nist.gov/kinetics/.